Initial Development of a High-frequency EMI Sensor for Detection of Subsurface Intermediate Electrically Conductive (IEC) Targets

Janet E. Simms[1], John B. Sigman[2], Benjamin E. Barrowes[3], Hollis H. Bennett Jr.[4], Donald E. Yule[1], Kevin O'Neill[2] and Fridon Shubitidze[2]
[1]U.S. Army Engineer Research and Development Center, Geotechnical and Structures Laboratory, 3909 Halls Ferry Road, Vicksburg, MS 39180
Email: janet.e.simms@usace.army.mil
[2]Thayer School of Engineering, 14 Engineering Drive, Dartmouth College, Hanover, NH 03755
Email: John.B.Sigman.TH@dartmouth.edu
[3]U.S. Army Engineer Research and Development Center, Cold Regions Research and Engineering Laboratory, 72 Lyme Road, Hanover, NH 03755
Email: benjamin.e.barrowes@usace.army.mil
[4]U.S. Army Engineer Research and Development Center, Environmental Laboratory, 3909 Halls Ferry Road, Vicksburg, MS 39180

ABSTRACT

The U.S. military has developed and currently uses composite material munitions. These composite munitions are typically comprised of carbon fiber and, because of their low electrical conductivity, have a much lower electromagnetic induction signature, which makes them difficult to detect using traditional metal detecting methods. The term intermediate electrically conductive (IEC) is used to describe these lower conductivity materials, with conductivity, σ, typically in the range $10 < \sigma < 10^5$ S/m. The electromagnetic induction (EMI) relaxation response of carbon fiber munitions peaks in the low megaHertz range (<15 MHz), but above 100 kHz. Thus, detecting and characterizing these munitions for remediation on military ranges is problematic using available geophysical EMI sensors. This paper describes initial efforts in the development of a prototype frequency-domain EMI sensor with the goal of extending the measurement frequency range to 15 MHz.

Introduction

As military conflicts move toward urban areas, there is an increased need to reduce collateral damage, reduce human injuries, and minimize environmental impact. One solution that addresses these needs is the development and use of composite munitions, especially those composed of non-metallic composite materials. Carbon fiber is one material that is currently used in composite munitions. The carbon fiber material disintegrates into small fibers upon explosion, thus limiting the amount of collateral damage to the immediate surroundings. However, the development of these non-metallic munitions creates a new challenge for unexploded ordnance (UXO) detection at U.S. military ranges. The electromagnetic geophysical sensors used to detect UXO rely on the contrast in magnitude of the signatures of the munitions and the background environment, and the frequency at which an item is detectable. Existing sensors perform well, because conventional metallic munitions have an electrical conductivity that is typically eight to ten orders of magnitude greater than the surrounding soils. In contrast, non-metallic munitions have electrical conductivities in the range of tens to thousands of Siemens/meter (S/m), whereas metals are typically on the order of 10^6 S/m and higher. These lower conductivity materials are difficult to detect with existing geophysical sensors. The term intermediate electrically conductive (IEC) (Schubitidze *et al*., 2014) is used to describe the materials used in these emerging non-metallic munitions.

Electromagnetic induction (EMI) sensors, both frequency domain and time domain, are typical geophysical sensors used for the detection of UXO. The EMI sensors currently available operate in the range of tens of Hertz to about 100 kiloHertz (kHz), with the

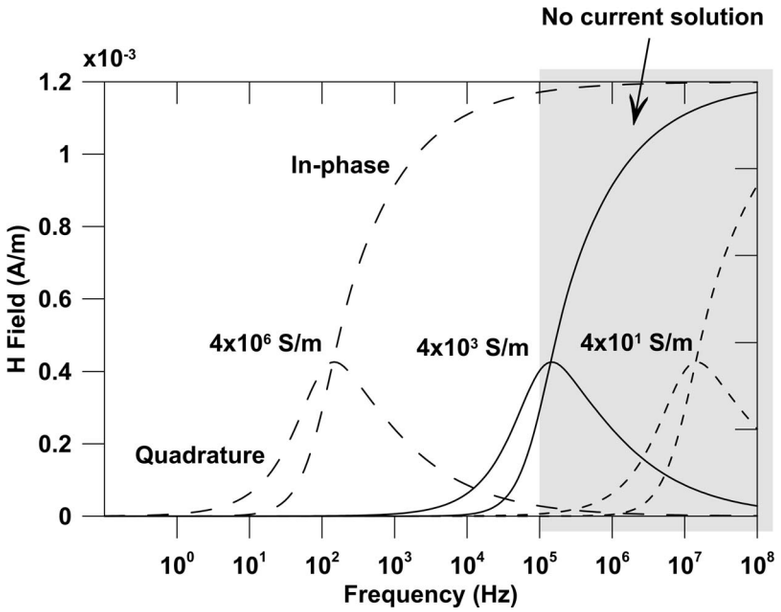

Figure 1. Model response (Wait, 1951; Wait and Spies, 1969) for a 10-cm conductive sphere ($\mu = 1$, $\varepsilon = 1$).

time-domain sensors not exceeding an equivalent 10 kHz. A metallic munitions' polarization relaxation response is within the signal detection range of the current low frequency EMI (LFEMI) geophysical sensors (below 100 kHz), and these sensors have proven effective for the detection and discrimination of metallic munitions. In contrast, carbon fiber material has a smaller signature magnitude at these low EMI frequencies, with a peak relaxation response occurring at higher frequencies (above 5 MHz) (see Fig. 1). Thus, emerging non-metallic munitions are essentially undetectable with current technologies developed for the detection and discrimination of metallic targets. A consideration in exploiting EMI for the detection of IEC munitions is the choice of time- or frequency-domain response approach. Because a time-domain EMI sensor's frequency response is limited by its turn off time, we concluded that to acquire EMI data at frequencies up to 15 MHz, a frequency-domain sensor is most suitable. Therefore, the goal of this research effort is to develop a prototype high frequency EMI (HFEMI) sensor capable of detecting IEC munitions.

Efforts to extend EMI sensing into the lower megaHertz range has progressed since the 1990s. Grover and Stewart (1990) and Stewart *et al*. (1990, 1994) developed the prototype High-Frequency Sounder (HFS), a frequency-domain instrument that operated in the range 300 kHz to 30 MHz. Transmitter–receiver spacing can vary between 0.5 m and 5 m, with a horizontal transmitter loop of radius 0.15 m and receiver consisting of two 0.15-m loops at right angles to sense the vertical and radial fields. To avoid issues regarding knowledge of the primary field and sensitivities to temperature fluctuations, the system uses the in-phase and quadrature measurements to calculate the tilt angle and ellipticity parameters of the magnetic field polarization ellipse. Research efforts at the Laboratory for Advanced Subsurface Imaging (LASI), University of Arizona, developed the LASI High-Frequency Ellipticity System (Sternberg and Pulton, 1991, 1994; Sternberg, 1999). This system operates in the frequency range 31 kHz to 32 MHz and uses multi-set transmitter (Tx) and receiver (Rx) square coils with varying side lengths (Tx max/min: 0.8/0.4 m; Rx max/min: 0.5/0.14 m) and coil turns (Tx max/min: 16/1; Rx max/min: 16/1) to allow data acquisition over the wide frequency band. The receiver has three-axis orthogonal coils and the ellipticity of the magnetic field is calculated. The transmitter–receiver separation is generally 2 to 8 m. Both the HFS and LASI systems acquire data while stationary because of the time required to complete a measurement. A comparable system in the time domain, the Very Early Time Electromagnetic (VETEM) system, is described by Pellerin *et al*. (1994, 1995, 1996), Wright *et al*. (1995, 1996), and Wright and Chew (2000). It allows faster data acquisition (less than 1 second per station) and

continuous profiling relative to the HFS and LASI systems. The VETEM has the option of three transmitters and three receivers. The transmitters include a 10.5-in. diameter loop with a preexisting programmable pulse length, 30-in. square loop with a programmable length ramp current, and an avalanche transistor pulser designed for use with the electric field dipole or 10.5-in. loop. The receivers include a linear receiver with a bandwidth from about 6 kHz to 70 MHz, linear receiver with a bandwidth of 20 kHz to 200 MHz designed for use with the electric field dipole antennas, and a linear/logarithmic receiver designed to improve the dynamic range of the receiver. A typical configuration is a horizontal transmitting loop and vertical receiving loop, spaced 2 m apart. Data presentation of the frequency- and time-domain systems described above is typically a 2-D frequency or time slice to obtain an image of the subsurface.

Carbon fiber-based fabrication has become more prevalent since the 1980's when it started to be used in high-end sports equipment. As manufacturing processes have matured, carbon fiber (CF) objects have grown in size and complexity, culminating in Boeing using CF for the entire fuselage of their new 777 "Dreamliner." New processes to detect defects in CF have also recently been developed (Salski *et al*., 2014; Heuer and Schulze, 2011). These non-destructive testing (NDT) techniques use induced eddy currents to detect structural and hidden defects such as missing carbon fiber bundles, lanes, suspensions, fringes, missing sewing threads and angle errors (Heuer and Schulze, 2011). These NDT techniques for CF use the same frequency range that our HFEMI instrument uses. However, the NDT instruments detect anomalies in the CF that are assumed to be of large extent (compared to the defect) and homogeneous.

In contrast, the HFEMI sensor we have developed is designed to acquire data over discrete targets to extract the electromagnetic relaxation signature. Our HFEMI instrument differs from the previously mentioned instruments in several areas including the scale under consideration, the intention of the instrument, and the assumptions regarding waves and the magneto-quasi-static (MQS) regime. The HFS instrument, for example, was specifically designed to acquire data related to "layered-earth models" in the "upper few meters" (Stewart *et al.,* 1990, 1994). This scale of the HFS (a few meters) is vitally different than a HFEMI instrument that acquires data only from objects and background that are closer than 50 cm to the instrument. The intention of the HFS is to survey bulk properties of the earth and thereby to infer information about electrical properties of the earth that are "important to agriculture, groundwater, waste disposal, archaeology, and soil engineering studies . . .". In contrast, the intention of our HFEMI instrument is to extract information from discrete inclusions in the soil, not the soil itself. The HFEMI instrument extracts in-phase and quadrature data from small targets (on the order of 30 cm) that are well under the minimum wavelength utilized (at 15 MHz: 20 m), whereas the HFS, LASI, and VETEM systems all operate over several meters depth of investigation. Similarly, the LASI system was also interested in "the variation of conductivity with depth" as well as the permittivity in the top several meters of the earth (Sternberg and Birkin, 1999; Sternberg *et al*., 1999). Finally, the VETEM instrument, in its several variations, employed antennas spaced multiple meters apart, with the goal of the investigation similar to that of the LASI instrument, *i.e*., bulk properties of the earth and images of these properties potentially revealing large metallic objects. These three prior systems were extensions of instruments such as the Geometrics EM31 and EM34, which survey~~ed~~ the earth for bulk properties with a range of several or dozens of meters, but ~~were~~ limited in frequency.

The HFEMI instrument described herein is an extension of the EMI UXO community, which came about from the early 2000s. This earlier research focused on using the EMI regime to investigate discrete metallic targets closer to the instrument, rather than extracting bulk properties of layered media on a larger scale (see Barrowes *et al*., 2015 for a review). The relaxation responses we report from discrete targets, in the tradition of Wait (Wait and Spies, 1969), allow the detection and discrimination of discrete, conductive and/or permeable inclusions in an otherwise slightly conducting background (typically the earth). Thus the scale, intention, and emphasis of our HFEMI instrument differ from the prior instruments operating in this frequency range.

At this point in our research, there is little concern regarding violation of Federal Communications Commission (FCC) regulations. FCC compliance of the HFEMI instrument in the low MHz range can be inferred from the fact that our system uses only 200 mA and a 25-cm diameter primary coil compared to the 1 A of current and 80-cm square coil of the LASI instrument. As field trials progress, radiated fields can be measured, as per Sternberg (1999), to ensure compliance.

This paper presents the initial sensor evolution and data acquired with the HFEMI sensor. There are still several issues to be investigated and resolved. Research continues to improve the sensor design and a description of the final prototype will be presented in a later paper.

Electromagnetic Induction Considerations

The skin depth, $\delta = \sqrt{(2/\omega\mu\sigma)}$, where $\omega = 2\pi f$ is the angular frequency (rad/s), μ is the magnetic permeability ($\mu \approx \mu_0 = 4\pi \times 10^{-7}$ H/m), and σ is the electrical conductivity (S/m), is a commonly used measure for the penetration of electromagnetic waves into conducting media. It is the depth at which the amplitude of the electric or magnetic field is reduced to $1/e$ (*i.e.*, 37%) of its surface value. For soil conductivities in the range of 0.001 to 0.1 S/m, the standard geophysical EMI sensors have skin depths ranging from about 5 km at the lowest frequency to 5 m at the higher frequencies. These lengths make the ground essentially transparent when searching for objects, especially at the lower frequencies and for metallic targets, whose conductivity is greater by nine orders of magnitude. Displacement currents in the soil can also be neglected, because the ratio of their magnitude to that of the conduction currents is on the order of $\delta^2/\lambda^2 \sim 10^{-6}$ (λ is wavelength) for the numbers quoted above (O'Neill, 2016).

The maximum depth at which a metallic or IEC target can be detected is based on the same principles regardless of the materials. The amplitude of magnetic fields under the MQS approximation fall-off as $1/R^3$, both between the primary coil and the object and the object and the receiver coil. This combined $1/R^6$ fall-off limits the range of detection of discrete targets. Beyond this well-known fall-off in secondary field response (O'Neill, 2016), the response from less conductive targets suffer from smaller eddy currents than those in metallic targets given the same excitation field. At the same time, this high frequency response benefits from greater dB/dt with the effect that the responses are on the same order. Data acquired from the HFEMI instrument over both a metallic target and a CF target simultaneously show that the in-phase and quadrature responses were similar in magnitude (Shubitidze *et al*., 2016; Barrowes *et al*., 2016), even though the metallic target had considerably more mass and volume. For this same reason of rapid fall-off with distance, discrete conducting targets greater than 50–100 cm away from the instrument will not contribute to the received signal.

Prior to designing a new sensor, it is necessary to understand the general signal response range of an IEC target. Wait's solution (Wait, 1951; Wait and Spies, 1969) for a conductive sphere within a low conductivity medium was used to model the response. Figure 1 shows the theoretical in-phase and quadrature responses for three 10-cm diameter spheres having conductivities 40, 4×10^3, and 4×10^6 S/m. The peak quadrature response of the 40 S/m sphere occurs at about 15 MHz, indicating that frequency-domain measurements are feasible for targets with conductivities in the tens of S/m range. At this frequency, wavelengths are on the order of 20 m, which is still long relative to the length scales in question ($<$1 m). Displacement currents also are still small in the soil compared to currents in the target, so the ground can be expected to remain "transparent" in the low MHz EMI range.

There are four main factors influencing the relaxation peak in Fig. 1: target size, target shape, magnetic permeability, and electrical conductivity. As target size increases, the relaxation peak shifts lower in frequency, whereas a change in target shape is not easily quantified and can shift the peak to either a higher or lower frequency. An increase in magnetic permeability or electrical conductivity shifts the peak to a lower frequency, and likewise, a decrease in permeability or conductivity shifts the peak to a higher frequency.

Modeling Sensor Performance

A modeling study is used to guide the design of the frequency-domain EMI system for detection and discrimination of subsurface IEC targets. This initial investigation is critical in understanding the response from complex IEC targets and nearby clutter. The clutter could include geologic clutter, such as permeable and/or conductive soils and rocks, as well as man-made metallic clutter. From the modeling effort, we will also gain understanding about the limits of high-frequency EMI technology as it relates to factors such as burial depth, environmental parameters, and clutter tolerance. The new sensing modality being developed will have practical performance issues that need to be understood, for example 1) What is the expected signal-to-noise ratio of this sensing modality in benign and more realistic conditions?, and 2) What type of transmitter and receiver configurations and combinations will be most useful in this frequency range to achieve the best detection and discrimination capabilities in geologically complex and cluttered environments? These initial investigations will aid in designing the prototype instrument.

A 3-D numerical model, the method of auxiliary sources (MAS) (Shubitidze *et al*., 2002, 2004, 2011), is used to understand EM induction phenomena for IEC targets in a wideband EMI frequency range (10 Hz to 15 MHz). The MAS approach was designed for solving electromagnetic radiation and scattering problems, and was selected because it is robust, easy to implement, and accurate. MAS derives its name from the use of auxiliary

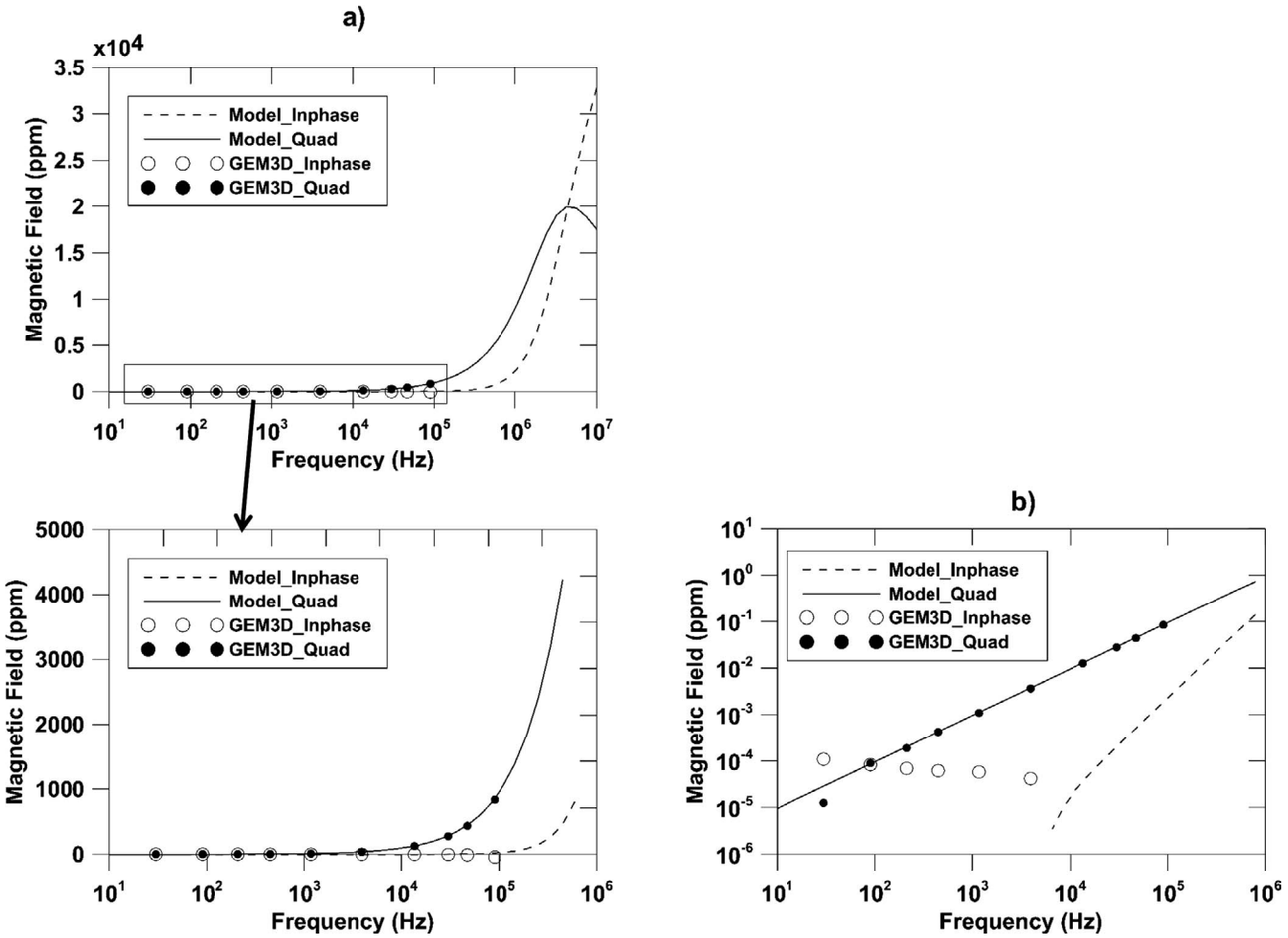

Figure 2. MAS model fit to frequency-domain EMI data (GEM-3D+) acquired over a five gallon bucket filled with a saturated $CaCl_2$ solution with conductivity estimated through simulation to be 20 S/m. Plots in a) show the traditional semi-log graphs, while b) has a log y-axis. In the MAS model, the solution was assigned a small non-zero permeability, which generated negative in-phase values below 10^4 Hz.

sources (elementary dipoles, charges, or currents) positioned on auxiliary surfaces, which conform to the material boundaries in the model. The auxiliary sources are represented numerically by a finite linear combination of analytical solutions of boundary value problems (relevant field equations) that represent the electromagnetic fields in each domain of the object. The method only requires points on the auxiliary and actual surfaces, so it is not necessary to resort to the detailed mesh structures required by finite-element or boundary-element methods.

The MAS model fit to the LFEMI sensor GEM-3D+ (Barrowes and O'Neill, 2010) data in Fig. 2 shows that the MAS is an acceptable technique for modeling frequency-domain EMI data. The data were acquired in air with the sensor resting on top of a plastic five gallon bucket containing approximately 20 S/m calcium chloride brine. The modeled quadrature peak occurs at around 4 MHz. In this data plot and the ones that follow, the EMI response is presented on a linear y-axis scale. Past and current literature on EMI responses for discrete conducting targets have almost universally presented in-phase and quadrature results on semi-log plots. The range of x-axis is log because of the broad frequency range and effects which scale as the square root of frequency. Y-axis results are usually linear because of the interesting behavior that occurs around the relaxation peak. When EMI is used to investigate bulk targets like bulk soil conductivity, results can be plotted on a log-log graph similar to Fig. 2(b) because the secondary field typically scales linearly (in log-log) with frequency. EMI data over discrete targets is usually presented as a semi-log graph similar to our Figs. 1, 2(a), 3, 4, and 6. These results for a less conducting discrete target could be

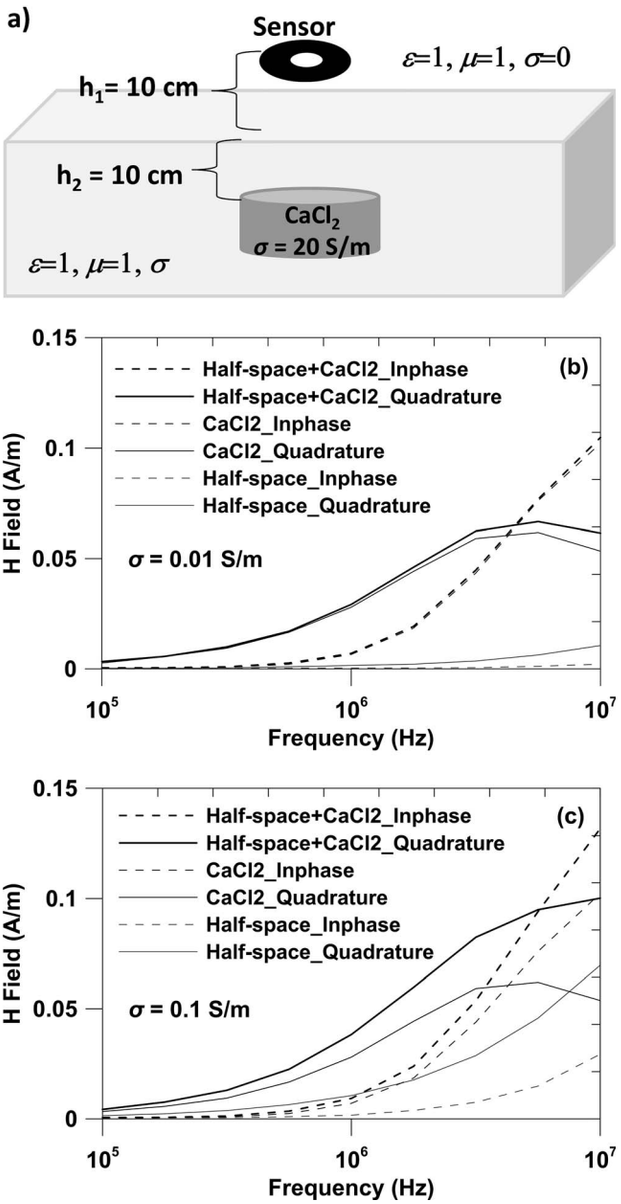

Figure 3. Influence of background conductivity on the ability to detect a buried IEC target. a) Model parameters. $CaCl_2$ bucket dimensions: radius 12.5 cm, height 38.5 cm; b) background conductivity $\sigma =$ 0.01 S/m; and c) background conductivity $\sigma = 0.1$ S/m.

plotted either as semi-log or log-log since a large, low conducting discrete target bridges the gap between a discrete high conducting target (like a UXO) and a very low conducting bulk target (soil half-space). We have presented both types of plots in Fig. 2, but will restrict ourselves to semi-log plots for the rest of the paper. A recent book by SPIE press on discrete target EMI (O'Neill, 2016) is a good background source regarding plots of this type.

The influence of the background medium (*i.e.*, soil) on an IEC target is shown in Fig. 3. The MAS models of the EMI response of a half-space (conductivities of 0.01 and 0.1 S/m), calcium chloride filled bucket ($\sigma = 20$ S/m) in air, and calcium chloride filled bucket in a half-space are shown. The EMI response is negligible for a low conductivity soil (Fig. 3(b)), whereas a high conductivity soil can screen the target signal (Fig. 3(c)).

Prototype Sensor Design

Basic Sensor Considerations

Because the peak quadrature response of IEC materials is in the low megaHertz (<15 MHz) range, it was decided that a frequency-domain sensor is needed. The initial components of the HFEMI sensor consisted of individual transmitter and receiver coils (Fig. 4), signal generator, oscilloscope, and computer. The signal generator creates the transmit current, and the oscilloscope synchronously logs the transmit current and receiver voltage waveforms. We typically chose to acquire data at 100 logarithmically-spaced frequencies between 500 Hz and 15 MHz.

EMI data for each new target require three measurements, *i.e.*, background (B), ferrite (F), and data (D). The background measurement is required to subtract out additive sources of noise such as residual primary field, ground response, and self-response, which are superimposed on the measured data. The ferrite measurement is used to divide out multiplicative sources of noise. Multiplicative noise sources are ones multiplied into the receiver data rather than being added into the receiver data. For example, a delay from the amplifier would be in the form of an exponential response ($e^{i*\mathrm{Delay}*\cdots}$), which is multiplied into the receiver data. Thus, to cancel the inherent response of the receiver coil, the measured data is divided by the ferrite response. Note that the magnetic response of ferrite, which is magnetic and non-conductive, must be constant in the measured frequency band. The background is measured on site and subtracted on a frequency-by-frequency basis, while the ferrite measurement is measured in air once for each new instrument geometry.

For measurements of intermediate conductivity materials of nominal size, frequencies up to 15 MHz should be used. The minimum wavelength in this frequency range is 20 m. Therefore, all of the sensing and data processing are developed assuming the magneto-quasistatic (MQS) approximation, which must hold approximately true for the entire frequency

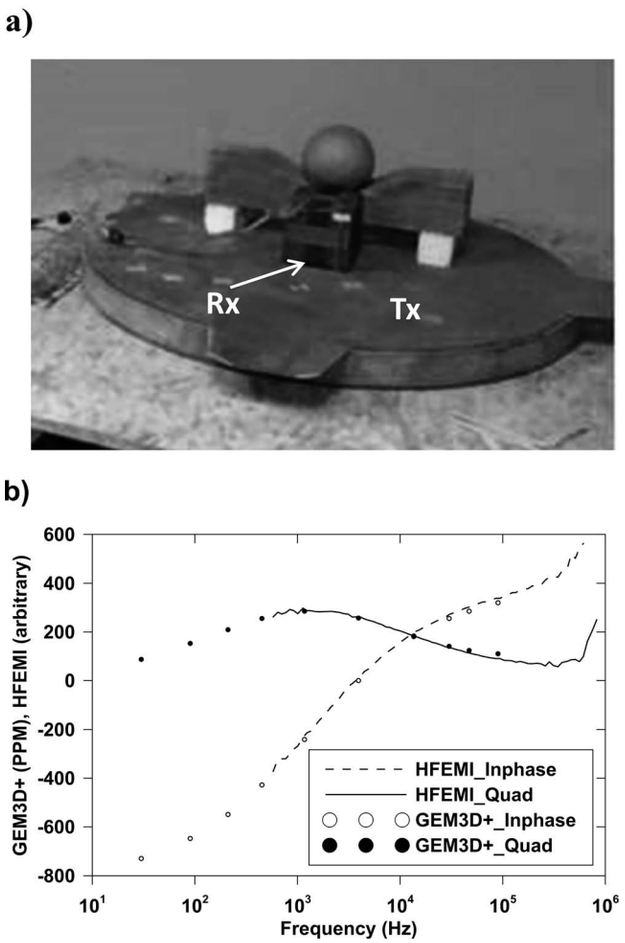

Figure 4. a) Photograph of the initial prototype HFEMI sensor (Tx coil: 14-turn, 75-cm diameter; Rx coil: early MPV 3-axis, 10-cm side cube with 100 turns) and b) data acquired with it compared to that acquired with the GEM-3D+ LFEMI sensor. Target is a 10.16-cm (4-in.) steel shot put.

bandwidth. A premise of the MQS approximation is that the currents at every point on the transmitter and receiver loops are at a single phase and directly proportional to the current measured by the instrument. If this is true for all frequencies, the spatial distribution of the primary field given by Ampere's law will be identical and proportional to the current measured. This is important for isolating an object's (whose location is unknown) response across the frequency bandwidth. These properties result in a receiver response that is flat and in-phase for all of the frequencies in our range of interest. Therefore, when the ferrite is measured, any deviation from a flat response is assumed to be caused by the inherent response of the receiver hardware. To compensate for the receiver hardware effects, we divide the data measurements by the measured ferrite response. For a more detailed treatment of the theoretical considerations of our prototype instrument, please see Sigman *et al*. (2016).

Sensor Configuration

The initial sensor design employed a large-diameter (75-cm), 14-turn coil for the transmitter, and a receiver cube borrowed from the man-portable vector (MPV) system (Barrowes *et al*., 2007). The receiver cube is a 3-axis, 10-cm side cube with 100 turns. Figure 4 shows the sensor and data acquired over a 10.16-cm (4-in.) steel shot put with the prototype HFEMI sensor. It is comparable to data (Grant *et al*., 2014) acquired with a LFEMI sensor (GEM-3D+, Barrowes and O'Neill, 2010). At this stage, the prototype sensor is only capable of reliable measurements up to 500 kHz. In this and subsequent figures showing HFEMI data, the vertical axis is in arbitrary units. This reflects the fact that we have not yet performed absolute (Amps/meter) or relative (parts per million) level calibration with the HFEMI instrument. The HFEMI data in Fig. 4 were scaled with one scale factor for both the in-phase and quadrature components to match the GEM-3D+ data. The same scale factor for both components produced HFEMI data that agreed qualitatively with the GEM-3D+ data in terms of the shape of the response as a function of frequency. Further calibration will be necessary for HFEMI data interpretation with respect to other instruments.

This first HFEMI prototype suffered from high noise, especially at the higher frequencies because of coil length considerations. This noise problem appears when the length of the coil approaches 2% of the free-space wavelength at the frequency of operation (Sigman *et al*., 2016). As a partial solution, our second design (Fig. 5) uses the same 14-turn transmitter coil, but the receiver was replaced with a figure-eight coil that has two 8-turn, 15.24-cm (6-in.) diameter loops, separated by 2.54 cm (1 in.). This quadrupole design provides geometric nulling of the primary field because the windings are in opposite directions. This figure-eight design was chosen as a quick and efficient method of nulling the primary field while also maintaining a short coil length. Oppositely wound coils such as those used in the GEM-3 might be more sensitive, but increased the length of the coil and added unnecessary complication at this early stage of design. We also added a current probe to more accurately measure the current as it enters the transmitter coil.

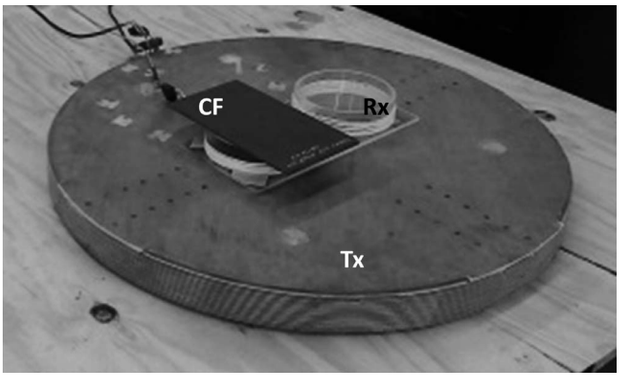

Figure 5. HFEMI prototype sensor with 14-turn Tx coil (diameter 75 cm) and 8-turn figure-eight Rx coil (diameter of each half is 15.24 cm (6 in.) with a 2.54-cm (1-in.) gap in between). Target is a 24.77-cm×13.65-cm×4.15-mm (9.75-in.×5.375-in.×0.16-in.) carbon fiber (CF) plate.

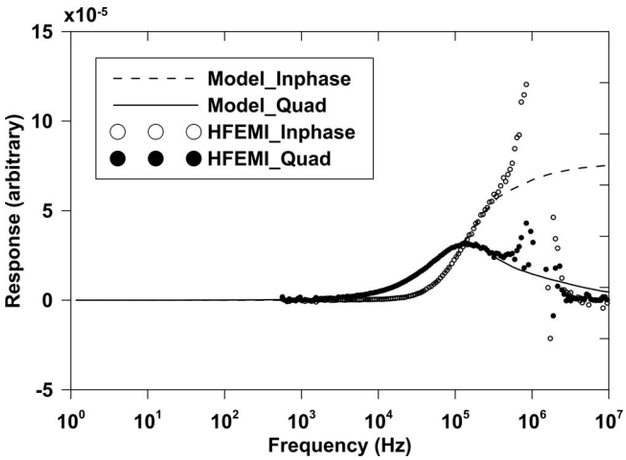

Figure 6. Carbon fiber plate (4-mm thickness) data acquired using the HFEMI prototype sensor compared to MAS model data. HFEMI system is that shown in Fig. 5.

Preliminary Results

The prototype HFEMI sensor shown in Fig. 5 was used to measure the response of a carbon fiber plate (Fig. 6). The data agree well with the MAS model up to 500 kHz. The estimated conductivity of the carbon fiber plate is 4,000 S/m, which was determined by adjusting the model fit to the data. This value for the conductivity of the CF plate is within the reasonable range for CF, but we have not tested the conductivity of the CF plate by other means. Yet it is encouraging that our instrument yielded reasonable estimates for the conductivity and may even become a way to measure the conductivity of IEC materials in the future. The instability in the data at higher frequencies is caused by LC resonances between the cables and the coils as well as the long electrical length of the coils. Further explanation of these issues is provided in Sigman *et al*. (2016). These data represent the first HFEMI relaxation response measurements for IEC targets in this frequency range. This type of relaxation spectra for IEC materials can be used, in a similar way to LFEMI signatures for metallic targets, to detect and discriminate between IEC discrete targets.

Conclusions

The development by the military of predominantly non-metallic munitions comprised of intermediate electrically conductive (IEC) materials (tens to thousands of S/m) has motivated the need for the development of a high frequency (<15 MHz) electromagnetic induction sensor. Previous EMI sensors operated in a frequency range with an upper limit of 100 kHz (GEM-3). A prototype HFEMI sensor was developed that is currently capable of reliable measurements from 500 Hz to 500 kHz. This HFEMI sensor is the first to acquire relaxation response EMI signatures from discrete low conducting targets in a similar manner to LFEMI sensors and metallic targets. This new HFEMI sensor consists of a 14-turn, 75-cm diameter transmitter coil and an 8-turn, figure-eight receiver coil (each half is 15.24-cm diameter with a 2.54-cm gap between coils). Data were successfully acquired for a carbon fiber plate, which is a common material for non-metallic munitions, and the data agree well with a numerical simulation of the plate based on the MAS model. Future efforts include calibrating the sensor against known targets, fully understanding the sources of noise in the system, and extending the reliable data measurement range to 15 MHz, which will likely be accomplished by modifying the transmitter and receiver coil configurations.

Acknowledgements

Funding for this research was provided by the EQ/I program, U.S. Army Engineer Research and Development Center. Permission to publish was granted by Director, Geotechnical & Structures Laboratory, U.S. Army Engineer Research and Development Center, Vicksburg, MS.

References

Barrowes, B.E., O'Neill, K., George, D., Snyder, S., and Shubitidze, F., 2007, Standardized excitations approach applied to man portable vector (MPV) time domain data: UXO Forum, August 2007, Orlando, FL.

Barrowes, B.E., and O'Neill, K., 2010, Handheld frequency domain vector EMI sensing for UXO discrimination: SERDP Project MM-1537, Final Report, 169 pp, https://www.serdp-estcp.org/Program-Areas/Munitions-Response/Land/Sensors/MR-1537/MR-1537.

Barrowes, B.E., Fernández, J.P., O'Neill, H., Shamatava, I., and Shubitidze, F., 2015, Electromagnetic induction tools for discrimination of unexploded ordnance: From basic physics to blind tests: *Fast*TIMES, **20**, 13–30.

Barrowes, B.E., Sigman, J.B., O'Neill, K., Simms, J.E., Bennett Jr., H.H., Yule, D.E., and Shubitidze, F., 2016, Detection of conductivity voids and landmines using high frequency electromagnetic induction: XXIth International Seminar/Workshop Direct and Inverse Problems of Electromagnetic and Acoustic Wave Theory DIPED.

Grant, S.A., Barrowes, B.E., Shubitidze, F., and Arcone, S.A., 2014, Homemade explosives in the subsurface as intermediate electrical conductivity materials: A new physical principle for their detection: *in* Detection and Sensing of Mines, Explosive Objects, and Obscured Targets XIX, Bishop, S.S. and Isaacs, J.C. (eds.), Proceedings of SPIE, **9072**, 90720A.

Grover, T.P., and Stewart, D.C., 1990, Short wave loop-loop sounder: U.S. Geol. Survey Open-File Report 90-318.

Heuer, H., and Schulze, M.H., 2011, Eddy current testing of carbon fiber materials by high resolution directional sensors: *in* Proceedings International Workshop Smart Materials, Structures & NDT in Aerospace, NDT in Canada.

O'Neill, K., 2016, Discrimination of subsurface unexploded ordnance: SPIE Press, Bellingham, Washington.

Pellerin, L., Labson, V.F., Pfeifer, M.C., and others, 1994, VETEM—a very early time electromagnetic system: *in* Proceedings of the Symposium on the Application of Geophysics to Engineering and Environmental Problems, 795–802.

Pellerin, L., Labson, V.F., Pfeifer, M.C., and others, 1995, VETEM—a very early time electromagnetic System—the first year: *in* Proceedings of the Symposium on the Application of Geophysics to Engineering and Environmental Problems, 725–731.

Pellerin, L., Pfeifer, M.C., Labson, V.F., and others, 1996, VETEM—a very early time electromagnetic system—Year 2: *in* Proceedings of the Symposium on the Application of Geophysics to Engineering and Environmental Problems, 91–95.

Salski, B., Gwarek, W., and Korpas, P., 2014, Electromagnetic inspection of carbon-fiber-reinforced polymer composites with coupled spiral inductors: IEEE Transactions on Microwave Theory and Techniques, **62**(7) 1535–1544.

Shubitidze, F., O'Neill, K., Haider, S.A., Sun, K., and Paulsen, K.D., 2002, Application of the method of auxiliary sources to the wide-band electromagnetic induction problem: IEEE Transactions on Geoscience and Remote Sensing, **40**(4), 928–942.

Shubitidze, F., O'Neill, K., Sun, K., and Paulsen, K.D., 2004, Investigation of broadband electromagnetic induction scattering by highly conductive, permeable, arbitrary shaped 3-D objects: IEEE Transactions on Geoscience and Remote Sensing, **4**(3) 540–556.

Shubitidze, F., Fernández, J.P., Barrowes, B.E., Shamatava, I., and O'Neill, K., 2011, The method of auxiliary sources for solving low-frequency electromagnetic induction problems in underwater environments: 27th International Review of Progress in Applied Computational Electromagnetics, Applied Computational Electromagnetics Society (ACES), New Electromagnetic Techniques and Measurements, Williamsburg, VA.

Shubitidze, F., Barrowes, B.E., Bennett, H.H., Sigman, J., Wang, Y., and O'Neill, K., 2014, Investigating EMI sensing phenomena for subsurface intermediate electrically conducting (IECM) target detection: *in* Proceedings: Symposium on the Application of Geophysics to Engineering and Environmental Problems, 484, doi: 10.4133/SAGEEP.27-167.

Shubitidze, F., Barrowes, B.E., Sigman, J.B., Simms, J.E., Bennett Jr., H.H., Yule, D.E., Shamatava, I., and O'Neill, K., 2016, Detection and discrimination subsurface low conducting buried hazards in a cluttered environment, *in* Proceedings Symposium on the Application of Geophysics to Engineering and Environmental Problems.

Sigman, J.B., Barrowes, B.E., O'Neill, K., Simms, J.E., Bennett, H.H., Jr., Yule, D.E., and Shubitidze, F., 2016, High-frequency electromagnetic induction sensing of non-metallic materials: IEEE Transactions on Geoscience and Remote Sensing, in review.

Sternberg, B.K., and Poulton, M.M., 1991, The LASI high frequency electromagnetic subsurface-imaging system: System description and demonstration site-characterization survey at the Idaho National Engineering Laboratory: U.S. Dept. of Energy's Morgantown Energy Technology Center, Contract No. DE-AC21-92MC29101 A001, pp. 18.

Sternberg, B.K., and Poulton, M.M., 1994, High-resolution subsurface imaging and neural network recognition: *in* Proceedings of the Symposium on the Application of Geophysics to Engineering and Environmental Problems, 847–855.

Sternberg, B.K., 1999, A new method of subsurface imaging—The LASI high frequency ellipticity system: Part 1. System design and development: Journal of Environmental and Engineering Geophysics, **4**(4) 197–213.

Sternberg, B.K., Thomas, S.J., and Birken, R.A., 1999, A new method of subsurface imaging—The LASI high frequency ellipticity system: Part 2. Data processing and interpretation: Journal of Environmental and Engineering Geophysics, **4**(4) 215–226.

Sternberg, B.K., and Birken, R.A., 1999, A new method of subsurface imaging—The LASI high frequency ellipticity system: Part 3. System tests and field surveys: Journal of Environmental and Engineering Geophysics, **4**(4) 227–240.

Stewart, D.C., Anderson, W.L., Grover, T.P., and Labson, V.F., 1990, New instrument and inversion program for near-surface mapping: High-frequency EM sounding and profiling in the frequency range 300 kHz to 30 MHz: *in* Expanded Abstracts: 60th Annual International Meeting and Exposition, Society of Exploration Geophysicists, 410–413.

Stewart, D.C., Anderson, W.L., Grover, T.P., and Labson, V.F., 1994, Shallow subsurface mapping by electromagnetic sounding in the 300 kHz to 30 MHz range: Model studies and prototype system assessment: Geophysics, **59**(8) 1201–1210.

Wait, J.R., 1951, A conducting sphere in a time varying magnetic field: Geophysics, **16**, 666–672.

Wait, J.R., and Spies, K.P., 1969, Quasi-static transient response of a conducting and permeable sphere: Geophysics, **34**, 789–792.

Wright, D.L., Grover, T.P., Labson, V.F., Pellerin, L., Ellefsen, K.J., and Bradley, J.A., 1995, Tomography between wells, a transient dielectric logging tool, and the very early time electromagnetic (VETEM) system: *in* Proceedings of the Symposium on the Application of Geophysics to Engineering and Environmental Problems, 501–510.

Wright, D.L., Grover, T.P., Labson, V.F., and Pellerin, L., 1996, The very early time electromagnetic (VETEM) system: First field test results: *in* Proceedings of the Symposium on the Application of Geophysics to Engineering and Environmental Problems, 81–90.

Wright, D.L., and Chew, W.C., 2000, Final report. Enhancements to and characterization of the Very early Time Electromagnetic (VETEM) prototype instrument and applications to shallow subsurface imaging at sites in the DOE Complex: U.S. Geological Survey, Denver, CO, 69 pp.

Queries for eego-22-02-02

1. Author, please provide DOI. Stylemarker